Applied Catalysis B: Environmental 338 (2023) 123000

Contents lists available at ScienceDirect

Applied Catalysis B: Environmental

journal homepage: www.elsevier.com/locate/apcatb

WO_3 boosted water tolerance of Pt nanoparticle on SO_4^{2-}-ZrO_2 for propane oxidation

Xu-Fang Wang, Lin-Ya Xu, Cai-Hao Wen, Dan-Dan Li, Bei Li, Ji-Qing Lu, Qi-Hua Yang, Meng-Fei Luo *, Jian Chen *

Key Laboratory of the Ministry of Education for Advanced Catalysis Materials, Zhejiang Key Laboratory for Reactive Chemistry on Solid Surfaces, Institute of Physical Chemistry, Zhejiang Normal University, Jinhua 321004, China

ARTICLE INFO

Keywords:
H_2O poisoning
Platinum-based catalyst
Propane complete oxidation
Strong metal-support interaction
Active site

ABSTRACT

H_2O poisoning of platinum-based catalysts for VOCs oxidation is a long-standing problem due to H_2O strongly competitive adsorption on active sites. In this work, it is found that the H_2O competitive adsorption on Pt active sites is effectively weakened by enhancing strong metal-support interaction (SMSI) in Pt-based catalyst. SMSI between WO_3 and Pt species occurs in the WO_3 supported Pt catalyst (Pt/WO_3) but disappears in Pt-3W/ZrO_2 due to monolayer dispersed WO_3 on ZrO_2. The formation of aggregated WO_3 species in Pt-3W/SO_4^{2-}-ZrO_2 leads to the SMSI which is further enhanced by SO_4^{2-}-ZrO_2. The enhanced SMSI plays critical role on weakening water vapor adsorption on active sites, thus Pt-3W/SO_4^{2-}-ZrO_2 exhibits both highest activity (T_{90} = 200 °C) and water tolerance which is much superior than Pt/ZrO_2, Pt/WO_3, Pt-3W/ZrO_2 and Pt/SO_4^{2-}-ZrO_2 under wet condition (5% H_2O). Our primary results provide a promising strategy for designing superior platinum catalysts for VOCs complete oxidation.

1. Introduction

Some of the most crucial performance indicators required for practical heterogeneous catalysts include excellent activity, durability, and poison resistance. Much effort has been devoted to developing high-performance catalysts for volatile organic compounds (VOCs) oxidation [1–5]. It is widely recognized that heterogeneous catalysts based on platinum group metals typically exhibit excellent catalytic activity, but are susceptible to serious deactivation from water vapor and substances containing heteroatoms (S, Cl) due to their strong adsorption properties. This is particularly true for the complete oxidation of VOCs, which contain various and complex compounds. In response to the pressing environmental concerns, significant research efforts have been dedicated to fundamental studies aimed at improving the catalytic activity and stability of platinum group catalysts used in the field of catalytic VOCs oxidation. Numerous studies have been conducted on the catalytic complete oxidation of saturated light alkanes such as methane and propane, due to their stable structure and widespread presence in exhaust gas from petrochemical fields. Additionally, a significant amount of hydrocarbon emissions are produced during the cold-start period of diesel engine vehicles [6–8]. Studies have shown that platinum-based catalysts demonstrate superior activity for the complete oxidation of propane, but inferior activity for the complete oxidation of methane when compared to palladium-based catalysts [9]. Propane complete oxidation over platinum-based catalysts has been widely investigated to date as a representative intractable VOC, with particular focus on improving catalytic activity and stability and understanding reaction mechanisms.

There is a wealth of literature detailing the development of platinum-based catalysts with increased catalytic activity. The oxidation state and dispersion of platinum species are significantly affected by the support and promoter utilized, thus the effects of these factors on catalyst performance have garnered the most research attention [10–13]. Supports that contain abundant acid sites are typically beneficial in enhancing the catalytic activity of platinum catalysts, as they promote the reduction of platinum oxides or increase the oxidation resistance of metallic platinum species. Yoshida et al. investigated various supports (MgO, La_2O_3, Al_2O_3, ZrO_2, SiO_2, SiO_2-Al_2O_3 and SO_4^{2-}-ZrO_2) and found that the intrinsic reactivity of platinum species for propane complete oxidation is significantly increased with the increase in acid strength of the supports [10,14]. Consequently, numerous studies have focused on modifying SO_4^{2-} groups on supports such as Al_2O_3, CeO_2, ZrO_2, CeO_2-ZrO_2, and TiO_2

* Corresponding authors.
E-mail addresses: mengfeiluo@zjnu.cn (M.-F. Luo), jianchen@zjnu.cn (J. Chen).

https://doi.org/10.1016/j.apcatb.2023.123000
Received 27 March 2023; Received in revised form 25 May 2023; Accepted 13 June 2023
Available online 19 June 2023

in order to increase the catalytic activity of platinum catalysts [15–20]. The effect of SO_2 present in the feed gas on the performance of platinum catalysts has also been discussed, as the acidic gas can alter the state of the support or platinum species [21,22]. It is widely agreed that sulfate species promote the cleavage of C-C bonds and accelerate the propane complete oxidation reaction, although this still remains a topic of debate [23,24]. Besides, the SiO_2/Al_2O_3 ratio of silica-alumina zeolites also affects the surface acidity and changes the Pt particle size of catalyst for propane complete oxidation, Park et al. found Pt/HZSM-5 (SiO_2/Al_2O_3 = 150) with smallest Pt particles and largest external surface area which shows the highest oxidation activity for propane combustion [25]. Reducible transition metal oxides (MoO_3, Nb_2O_5, WO_3, V_2O_5, etc) are often employed as promoter to modulate the active sites thereby increasing the catalytic activities of platinum based catalysts for propane complete oxidation. [26–31]. Wu et al. found that electronic interactions between Pt and WO_x clusters lead to the generation of more active sites $Pt^{\delta+}$ species in Pt/WO_x/Al_2O_3 catalysts for propane oxidation [32]. Zhu et al. also found that more metallic platinum with high oxidation resistance generated by WO_3 modification and propane complete oxidation reaction was enhanced over Pt-W/ZSM-5 catalyst [33]. Our previous works revealed the critical role of Pt-MO_x (M= W, Mo) interface sites for propane complete oxidation, and tuned the interface sites density by changing preparation methods, and surface hydroxyl groups on WO_3 are also of great importance for propane complete oxidation.[22,25,26] However, there is rarely works investigating the role of SMSI between Pt species and reducible oxides on catalytic propane oxidation, which is the most pronounced character of reducible oxides supported Pt catalyst and widely studied in hydrogenation reaction [34,35].

H_2O poisoning as one of the most threat to platinum group based catalyst, many strategies have been provided for enhancing catalyst water tolerance. Increasing the SiO_2/Al_2O_3 ratio of ZSM-5 zeolite can efficiently improve the water tolerance of palladium catalyst because of the hydrophobic support [36]. Murata et al. also used the hydrophobic support (α-Al_2O_3) to reduce H_2O poisoning of supported PdO catalyst for methane combustion reaction [37]. Catalytic activity of palladium catalyst could be effectively maintained at high level for methane combustion through in situ water sorption by water sorbents [38]. Brønsted acid sites prevented water to cover on the Pt surface through a spillover-like mechanism, thus more Pt sites were available for propane adsorption and activation [39]. It can be seen that most of the reported methods considered to change the support properties rather than precisely regulated active sites structure to improve catalyst water tolerance. Usually, water vapor in feed gas deactivates platinum group based catalysts since it competes with reactant molecule for available adsorption active sites or leads to the remarkable aggregation of active sites [37,38,40–42]. How to effectively regulate the active sites structure and improve their water tolerance is very crucial. However, to the best of our knowledge, many previous works on VOCs complete oxidation exclude the addition of water to the reaction mixture and neglect the role of structural design of active sites on catalyst water tolerance.

Our previous work found that sulfate species remarkably promote C-C bond containing saturated alkane (ethane, propane, n-hexane) complete oxidation over Pt/SO_4^{2-}-ZrO_2 catalyst in comparison with bare Pt/ZrO_2 catalyst [43]. To be frustrated, the Pt/SO_4^{2-}-ZrO_2 catalyst suffers a significant deactivation for propane complete oxidation with water vapor (5% H_2O) in feed gas due to its strongly competitive adsorption on active sites. Herein, we found the different behavior of WO_3 aggregation on ZrO_2 (monolayer WO_3) and SO_4^{2-}-ZrO_2 (aggregated WO_3 island) surfaces, and Pt species loaded on this different WO_3 species surface show very different behaviors for water tolerance. Namely, the Pt-3W/SO_4^{2-}-ZrO_2 catalyst presents the highest water tolerance due to the weakened H_2O competitive adsorption with reactants when Pt species on the aggregated WO_3 island supported by SO_4^{2-}-ZrO_2.

2. Experimental section

2.1. Catalyst preparation

Pt/ZrO_2 and Pt/SO_4^{2-}-ZrO_2 catalysts were prepared according to the same method in our previous work.[43] ZrO_2 support was obtained by calcining the $ZrOCO_3$ at 500 °C. SO_4^{2-}-ZrO_2 support was prepared by immersing ZrO_2 support (2 g) into sulfuric acid solution (3 mL, 0.5 mol L^{-1}), then the solid was collected by centrifuging and dried at 100 °C for 12 h, followed by calcination in static air at 500 °C for 3 h. Typical impregnation method was adopted to load 2 wt% Pt on ZrO_2 and SO_4^{2-}-ZrO_2 support for preparation of Pt/ZrO_2 and Pt/SO_4^{2-}-ZrO_2 catalysts. 1 g support (ZrO_2 or SO_4^{2-}-ZrO_2) was added to aqueous solution of $Pt(NO_3)_2$ (10 mL, 0.002 mg L^{-1}), and the mixture was stirred at 35 °C for 3 h and evaporated at 90 °C. Then, the solid was dried in an oven at 100 °C for 5 h and calcined in static air at 500 °C for 4 h with a heat ramp of 10 °C min^{-1}.

Pt-3W/ZrO_2 and Pt-3W/SO_4^{2-}-ZrO_2 catalysts were prepared by co-impregnating $Pt(NO_3)_2$ and ammonium tungstate hydrate. The nominal loading of Pt and W is 2 and 3 wt%, respectively. Other steps are same to those for preparation of Pt/ZrO_2 and Pt/SO_4^{2-}-ZrO_2 catalysts. WO_3 support was obtained by calcinating ammonium tungstate hydrate in static air at 500 °C, and reference catalyst Pt/WO_3 was also prepared by impregnation method.

2.2. Characterization

Brunauer-Emmet-Teller (BET) surface areas of these catalysts were determined by N_2 adsorption in a BK200C system volumetric adsorption analyzer at 77 K. Prior to test, 100 mg of catalyst was dried at 100 °C for 12 h and degassed at 200 °C for 4 h. The actual Pt content in the catalyst was detected by X-ray fluorescence (XRF) analysis on a Shimadzu XRF-1800 spectrometer. The powder X-ray diffraction (XRD) pattern of catalyst was recorded on a Bruker D8 diffractometer with Cu K_α radiation operated at 40 kV and 40 mA, the scan speed was 12° min^{-1} at 2θ of 10–90°. To measure the Pt dispersion of catalyst, the CO chemisorption test was performed on the BELCAT II analyzer at 30 °C after the pre-reduction of catalyst in a flow (5%H_2 + 95%He) at 100 °C. Raman spectra were recorded by a confocal microprobe Raman system (Renishaw inVia Reflex) with an excitation laser of 325 nm (laser power =10 mW, dwell time = 60 s, number of scans = 100, resolution =1 cm^{-1}). NH_3-temperature programmed desorption (NH_3-TPD) experiment was also conducted on the home-made tubular quartz reactor equipped with a thermal conductivity detector (TCD). To clean the catalyst surface, the catalyst (200 mg, 60–80 mesh) was put in the reactor and pre-treated in a N_2 flow (20 mL min^{-1}) under 300 °C for 0.5 h, and cooled down to 50 °C. Then, high purity NH_3 gas was flowed in the reactor (30 mL min^{-1}) for 10 min, and N_2 flow (20 mL min^{-1}) was purged for 0.5 h to clean the gaseous or physically adsorbed NH_3 on catalyst. Then, the catalysts were heated from 40° to 700°C in a high purity N_2 flow (20 mL min^{-1}) to desorb the chemical adsorption NH_3, then outlet gas from the reactor was dehydrated by KOH and then introduced into TCD detector to record the NH_3 signal, calculating NH_3 desorption amount by fitting desorption peak area and using peak area of NH_3 in a quantitative ring as reference. High resolution transmission electron microscope (HRTEM) images of the catalysts were obtained on a JEOL-2100 F microscope operated at 200 kV. Diffuse reflectance infrared Fourier transform spectra (DRIFTS) of CO chemisorption, in situ propane and CO oxidation on the Pt catalysts were measured on a Thermal-Fischer Nicolet iS50 FT-IR spectrometer equipped with a MCT detector and a PIKE DRIFT accessory. X-ray photoelectron spectra (XPS) were obtained on an ESCALAB 250Xi instrument with Al K_α source. The binding energies (BEs) was calibrated by the carbonaceous C1s line (284.6 eV).

2.3. Catalytic activity evaluation

The activities of the catalysts for propane oxidation were measured in a tubular quartz reactor (*i.d.* = 6 mm). Typically, 50 mg of catalyst (60–80 mesh) diluted by 50 mg quartz sand was put in the reactor. For the dry condition, the feed gas consisted of 0.2 vol% C_3H_8 + 2 vol% O_2/N_2 balanced was flowed to the catalyst bed with a flow of 66.6 mL min^{-1} (mass space velocity of 80000 mL g^{-1} h^{-1}). For the wet condition, the mixture gas above went through a water bottle (water vapor partial pressure of 5.03 kPa) at 33.4 °C and was diluted by the 5% H_2O. The concentrations of propane in the inlet and outlet were detected by a gas chromatography (Shimadzu GC-2014) equipped with a DB-Wax (30 m × 0.25 mm × 0.25 μm) capillary column and FID detector.

$$\text{Propane conversion} = ([C]_{in} - [C]_{out})/[C]_{in} \times 100\%$$

$[C]_{in}$ and $[C]_{out}$ represents the propane concentration in inlet and outlet gas, respectively. No byproducts other than H_2O and CO_2 were detected by GC, CO_2 selectivity is close to 100%.

Propane complete oxidation reaction kinetics were performed at differential reaction condition (with propane conversion below 15%), see Supporting Information. The catalyst was diluted with quartz sand (with same size) to 100 mg, and it was aged under the same condition as in catalytic test. By adjusting the partial pressures of propane (0.202–0.808 kPa), O_2 (9.09–1.515 kPa) and H_2O (0.611–7.381 kPa) in the reaction gas, a series of reaction rates were obtained and related kinetic parameters were derived. The detailed data of Arrhenius plots are also given in Supporting Information for calculating apparent activation energy (Ea).

3. Result and discussion

3.1. General characterization

Table 1 summarizes the basic parameters of physical and chemical properties for the as-prepared Pt/ZrO_2, $Pt\text{-}3W/ZrO_2$, $Pt/SO_4^{2-}\text{-}ZrO_2$ and $Pt\text{-}3W/SO_4^{2-}\text{-}ZrO_2$ catalysts. The Pt/ZrO_2 and $Pt/SO_4^{2-}\text{-}ZrO_2$ catalysts are prepared by referring our previous work, [43] and low surface area of all these catalysts measured by N_2 adsorption is ascribed to the non-porous structure of ZrO_2 support. Pt and W actual content is consistent with the nominal value due to using impregnation method, and S content was introduced with 0.05 mmol g_{cat}^{-1} by controlling the H_2SO_4 impregnation amount as described in experiment section. By using CO as the probe molecule, CO chemical adsorption was conducted to determine the amount of exposed Pt sites accessible for CO. High CO uptake of the Pt/ZrO_2 catalyst suggests that Pt species is highly dispersed on ZrO_2 surface, whereas very low CO uptake observed on the reference catalyst Pt/WO_3 is ascribed to the SMSI between Pt species with reducible oxides WO_3, even though small Pt species particles are observed on Pt/WO_3 (Fig. S1) [44]. Compared to the Pt/ZrO_2 catalyst, the $Pt/SO_4^{2-}\text{-}ZrO_2$ catalyst shows very low CO uptake due to strong interaction between Pt and SO_4^{2-} species, even though Pt species geometric size are same for the Pt/ZrO_2 and $Pt/SO_4^{2-}\text{-}ZrO_2$ catalyst as discussed in our previous work. [43] Interestingly, the $Pt\text{-}3W/ZrO_2$ catalyst shows higher CO uptake than the Pt/ZrO_2 catalyst, but the $Pt\text{-}3W/SO_4^{2-}\text{-}ZrO_2$ catalyst shows lower CO uptake than the $Pt/SO_4^{2-}\text{-}ZrO_2$ catalyst. The above results suggest the interactions between WO_3 species and Pt species in the $Pt\text{-}3W/ZrO_2$ and $Pt\text{-}3W/SO_4^{2-}\text{-}ZrO_2$ catalysts are very different, which may be ascribed to effect from SO_4^{2-} species. It can be inferred that SMSI between Pt species with reducible oxides WO_3 is enhanced by $SO_4^{2-}\text{-}ZrO_2$, thereby resulting in the lowest CO uptake in the $Pt\text{-}3W/SO_4^{2-}\text{-}ZrO_2$ catalyst. Whereas, such SMSI disappears in the $Pt\text{-}3W/ZrO_2$ catalyst as evidenced by its highest CO uptake.

Table 1
Physical and chemical properties of the Pt/ZrO_2, $Pt\text{-}3W/ZrO_2$, $Pt/SO_4^{2-}\text{-}ZrO_2$ and $Pt\text{-}3W/SO_4^{2-}\text{-}ZrO_2$ catalysts.

Catalyst	BET Surface area (m^2 g_{cat}^{-1})	Element content[a]			CO uptake (μmol g_{cat}^{-1})[b]	D_{Pt} (%)[c]
		Pt (wt %)	S (mmol g_{cat}^{-1})	W (wt %)		
Pt/ZrO_2	18	1.9	0	0	36.8	35.9
Pt/WO_3	18	1.9	0	79.2	5.9	5.8
$Pt\text{-}3W/ZrO_2$	20	1.8	0	2.9	41.3	40.2
$Pt/SO_4^{2-}\text{-}ZrO_2$	18	1.9	0.05	0	6.9	6.7
$Pt\text{-}3W/SO_4^{2-}\text{-}ZrO_2$	22	1.8	0.05	2.8	2.3	2.3

[a] Element content was determined by XRF;
[b] CO uptake was determined by pulse chemical adsorption;
[c] D_{Pt} represents the ratio of Pt atoms that are available for CO molecule adsorption, which is determined through CO pulse chemical adsorption and calculated based on the CO capacity while assuming CO: Pt= 1:1.

Fig. 1a shows the XRD patterns of the Pt/ZrO_2, $Pt\text{-}3W/ZrO_2$, $Pt/SO_4^{2-}\text{-}ZrO_2$ and $Pt\text{-}3W/SO_4^{2-}\text{-}ZrO_2$ catalysts. No characteristic diffraction peaks assigned to Pt species and WO_3 are observed because of their low content or high dispersion. Only monoclinic phase m-ZrO_2 exists in the Pt/ZrO_2 and $Pt/SO_4^{2-}\text{-}ZrO_2$ catalysts, whereas a weak diffraction peak at 30.2° appears in the $Pt\text{-}3W/ZrO_2$ and $Pt\text{-}3W/SO_4^{2-}\text{-}ZrO_2$ catalysts which is ascribed to metastable tetragonal phase t-ZrO_2 [45,46]. This result suggests WO_3 species leads to the generation of metastable t-ZrO_2. Previous works also reported WO_3 species preferred to self-disperse as monolayer on ZrO_2 surface and stabilized the metastable t-ZrO_2. [47–49]. For the Raman spectra of the $Pt\text{-}3W/ZrO_2$ catalyst (Fig. 1b), a weak Raman vibration at 963 cm^{-1} can be ascribed to W=O symmetrical stretching vibration of monolayer WO_3 [50]. Raman vibration of crystalline.

phase WO_3 appears at 811 cm^{-1} for the $Pt\text{-}3W/SO_4^{2-}\text{-}ZrO_2$ catalyst, suggesting partial WO_3 species aggregated on the $SO_4^{2-}\text{-}ZrO_2$ surface in addition to those monolayer dispersed (at 970 cm^{-1}). This results confirm that sulfate species change the aggregation state of WO_3 on the ZrO_2 surface. NH_3-TPD profiles investigate the surface acidity of these catalysts as shown in Fig. 1c. Sulfate species remarkably increase surface acidity of ZrO_2 ($Pt/SO_4^{2-}\text{-}ZrO_2$ vs Pt/ZrO_2), WO_3 species slightly improve the surface acidity of ZrO_2 ($Pt\text{-}3W/ZrO_2$ vs Pt/ZrO_2). However, the decreased surface acidity is observed for the $Pt\text{-}3W/SO_4^{2-}\text{-}ZrO_2$ catalyst in comparison with $Pt/SO_4^{2-}\text{-}ZrO_2$ catalyst, which is ascribed to partial sulfate species on ZrO_2 covered by WO_3 species. Pt nanoparticles with Pt (111) face exposed are observed whereas no WO_3 particles can be found in the HRTEM image of $Pt\text{-}3W/ZrO_2$ catalyst (Fig. 1d),[17] further confirming that WO_3 is highly dispersed on the ZrO_2 surface, commonly regarded as monolayer. However, WO_3 particles with WO_3 (001) face exposed like island can be clearly observed on the $Pt\text{-}3W/SO_4^{2-}\text{-}ZrO_2$ catalyst and Pt nanoparticles are loaded on WO_3 island (Fig. 1d), suggesting there are aggregated WO_3 island on the ZrO_2 surface. Such very different structure may be responsible for the different behavior of CO adsorption on these two catalysts ($Pt\text{-}3W/ZrO_2$, $Pt\text{-}3W/SO_4^{2-}\text{-}ZrO_2$), namely, monolayer dispersed WO_3 favors the CO adsorption on Pt species but aggregated WO_3 suppresses the CO adsorption on Pt species due to SMSI between Pt species with reducible oxides WO_3. Furthermore, such SMSI can be enhanced on $SO_4^{2-}\text{-}ZrO_2$ support, thus the $Pt\text{-}3W/SO_4^{2-}\text{-}ZrO_2$ catalyst shows the lowest CO uptake.

3.2. Catalytic activity

Fig. 2 shows the catalytic activities of these catalysts for propane complete oxidation. Fig. 2a displays the light-off curves of propane complete oxidation over the Pt/ZrO_2, $Pt\text{-}3W/ZrO_2$, $Pt/SO_4^{2-}\text{-}ZrO_2$ and $Pt\text{-}3W/SO_4^{2-}\text{-}ZrO_2$ catalysts under dry condition. The catalytic activities of these catalysts are in order of $Pt/SO_4^{2-}\text{-}ZrO_2$ > $Pt\text{-}3W/SO_4^{2-}\text{-}ZrO_2$ > $Pt\text{-}3W/ZrO_2$ > Pt/ZrO_2. But very different activity order of these catalysts

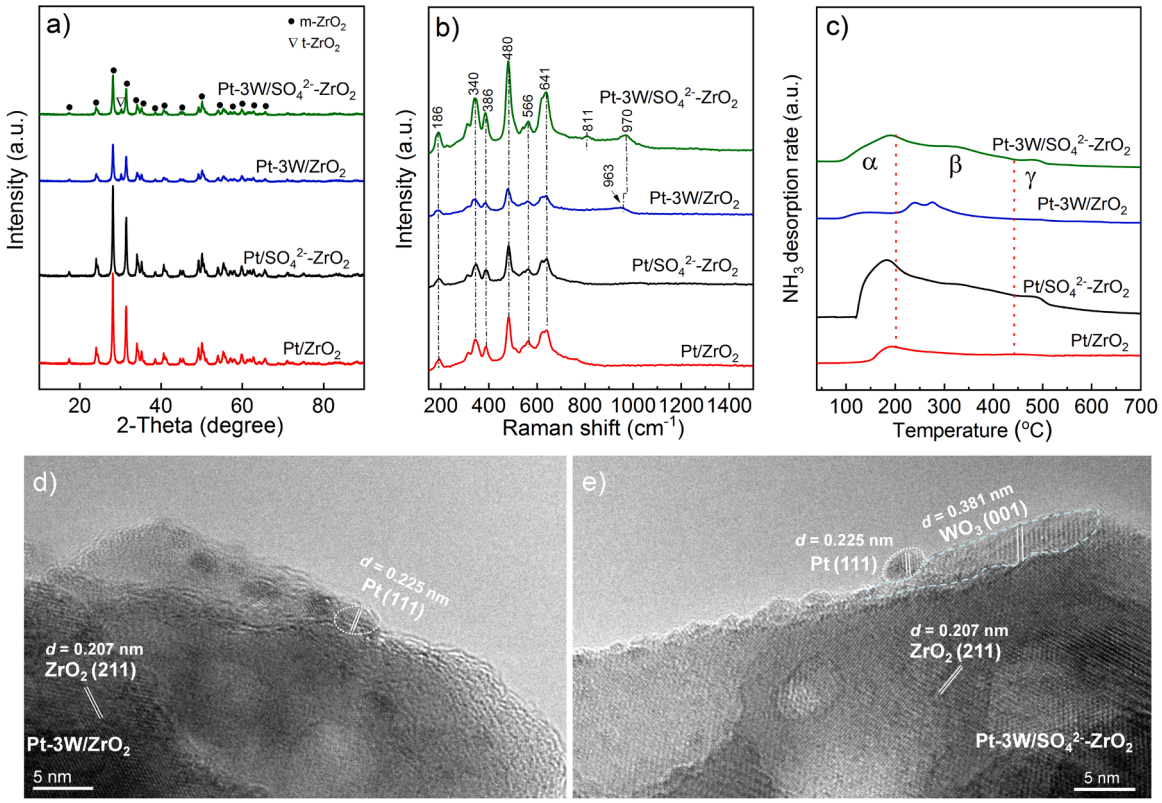

Fig. 1. a) The XRD patterns, b) Raman spectra and c) NH_3-TPD profiles of the Pt/ZrO_2, $Pt\text{-}3W/ZrO_2$, $Pt/SO_4^{2-}\text{-}ZrO_2$ and $Pt\text{-}3W/SO_4^{2-}\text{-}ZrO_2$ catalysts; HRETM images of d) $Pt\text{-}3W/ZrO_2$ and e) $Pt\text{-}3W/SO_4^{2-}\text{-}ZrO_2$ catalysts.

are observed under the wet reaction condition (5% H_2O) as shown in Fig. 2b. Under wet condition, the highest catalytic activity is obtained on the $Pt\text{-}3W/SO_4^{2-}\text{-}ZrO_2$ catalyst which is comparable to its activity under dry condition at high temperature (>250 °C). Whereas other three catalysts obviously are deactivated under wet condition. To directly observe the deactivation extent, propane oxidation reactions on these catalysts were conducted under staged conditions at 250 °C as shown in Fig. 2c-d. The Pt/ZrO_2 catalyst shows inferior catalytic activity under dry condition and remarkable deactivation under wet condition. Compared to the Pt/ZrO_2 catalyst, the $Pt\text{-}3W/ZrO_2$ catalyst has higher catalytic activity under dry condition but it also suffers remarkable deactivation under wet condition (Fig. 2c). This result suggests that monolayer dispersed WO_3 species in $Pt\text{-}3W/ZrO_2$ promotes the propane oxidation but it is ineffective to improve water tolerance of catalyst. In addition, the $Pt/SO_4^{2-}\text{-}ZrO_2$ catalyst shows higher catalytic activity compared to the $Pt\text{-}3W/ZrO_2$ catalyst, suggesting the superior promotion of SO_4^{2-} than WO_3 on catalytic oxidation activity. However, the $Pt/SO_4^{2-}\text{-}ZrO_2$ catalyst presents a intensive deactivation under wet condition, indicating its very poor water tolerance. Interestingly, the $Pt\text{-}3W/SO_4^{2-}\text{-}ZrO_2$ catalyst not only exhibits a very high catalytic activity under dry condition but also robust water tolerance under wet condition. To study the effect of WO_3 state (monolayer or aggregated particles) on the water tolerance of catalyst, the performance of reference catalyst Pt/WO_3 was also conducted under staged conditions at 250 °C as shown in Fig. S2. The Pt/WO_3 catalyst shows both superior activity and water tolerance compared to the $Pt\text{-}3W/ZrO_2$ catalyst. The above results confirm that Pt nanoparticles loaded on aggregated WO_3 island indeed improve the water tolerance of catalyst. Furthermore, the enhanced SMSI between Pt species with reducible oxides WO_3 in the $Pt\text{-}3W/SO_4^{2-}\text{-}ZrO_2$ catalyst may explain its superior water tolerance than the Pt/WO_3 catalyst. The influence of different humidity (0, 2.5, 5, 7.5% H_2O) on catalytic activity of representative catalyst of $Pt\text{-}3W/SO_4^{2-}\text{-}ZrO_2$ was also investigated (Fig. S3). It can be found that increasing humidity of feed gas hardly affects the catalytic activity of the $Pt\text{-}3W/SO_4^{2-}\text{-}ZrO_2$ catalyst at high reaction temperature (>250 °C) when water vapor below 5%, whereas excessively high humidity (such as 7.5% H_2O) remarkably decreases the catalytic activity, especially for low reaction temperature (<250 °C). This result can be attributed to the significantly competitive adsorption of H_2O with reactant molecule on the active sites of the catalyst under conditions of increased humidity or low reaction temperature.

In order to further study the stability of the $Pt\text{-}3W/SO_4^{2-}\text{-}ZrO_2$ catalyst, its catalytic activity for propane oxidation under wet condition for long period was conducted as shown in Fig. 3. It can be found that the catalytic activity of the $Pt\text{-}3W/SO_4^{2-}\text{-}ZrO_2$ catalyst could maintain as the fresh catalyst for a long time, suggesting the active site structure of catalyst is very robust under such reaction condition.

To further explain why these catalysts show different catalytic behaviors against water vapor, kinetic experiments were conducted on four representative catalysts (Pt/ZrO_2, $Pt\text{-}3W/ZrO_2$, $Pt/SO_4^{2-}\text{-}ZrO_2$ and $Pt\text{-}3W/SO_4^{2-}\text{-}ZrO_2$) as shown in Fig. 4 and Table 2. The derived power law rate expression of the overall propane oxidation reaction can be described as $r = k\,[P_{C3H8}]^a\,[P_{O2}]^b[P_{H2O}]^c$, k is apparent rate constant, a, b and c are the rate orders of propane, oxygen, and water, respectively.[39] This rate expression can directly identify the effect of water vapor on the reaction rate. The $Pt\text{-}3W/SO_4^{2-}\text{-}ZrO_2$ catalyst has the highest apparent rate constant, which is consistent with its superior catalytic activity as given in Fig. 2b. For the rate orders, all these catalysts present the rate order of propane close to one, due to propane molecule weakly adsorbing on catalyst surface. Negative rate order of O_2 is obtained for these catalysts, suggesting O_2 strongly adsorbs on active sites and shows competitive adsorption with propane. Compared to the Pt/ZrO_2, $Pt\text{-}3W/ZrO_2$ and $Pt/SO_4^{2-}\text{-}ZrO_2$ catalysts, this negative effect of O_2 competitive adsorption will be weakened for the $Pt\text{-}3W/SO_4^{2-}\text{-}ZrO_2$ catalyst. Importantly, these catalysts present very different rate orders for H_2O, the $Pt/SO_4^{2-}\text{-}ZrO_2$ catalyst shows the largest negative rate order of − 0.55 which

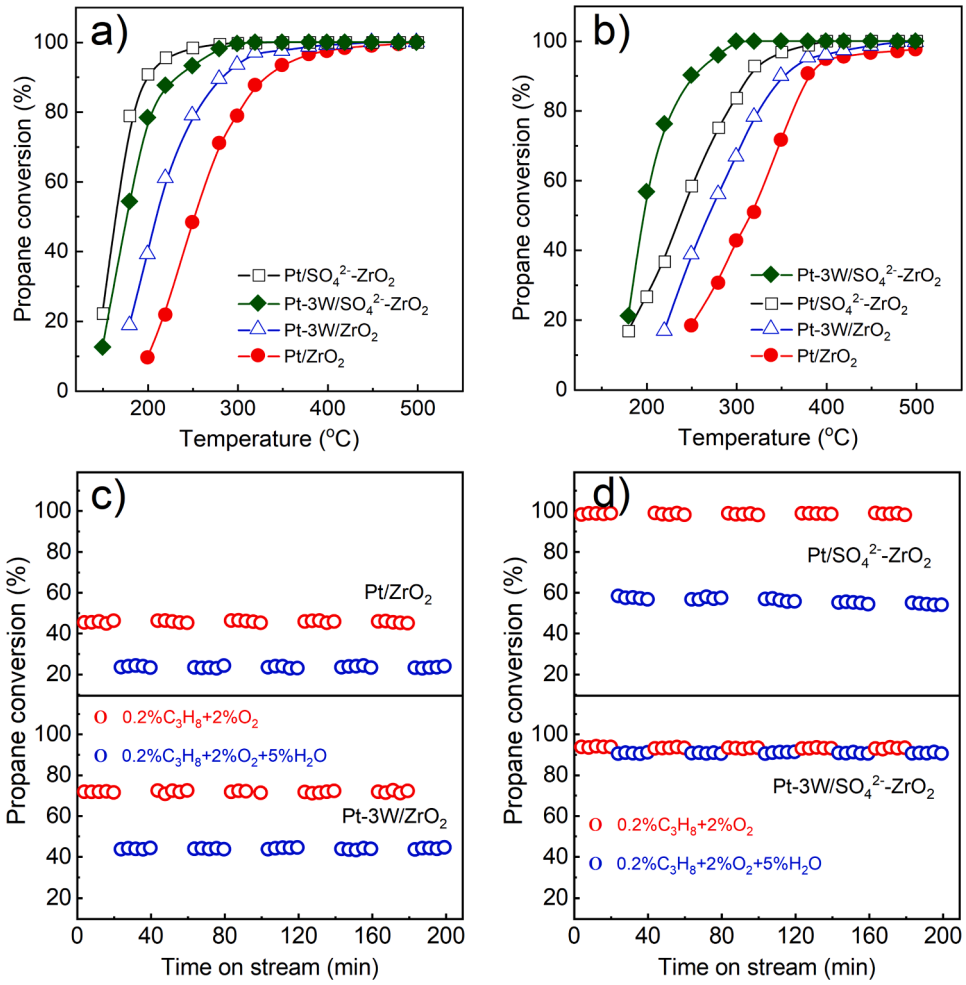

Fig. 2. Light-off curves of propane complete oxidation over catalysts under a) dry condition and b) wet condition with 5% H_2O; c) and d) Propane oxidation activity of catalysts under staged conditions at 250 °C (o reaction condition: 0.2% C_3H_8 + 2% O_2/N_2 balanced; o reaction condition: 0.2% C_3H_8 + 2% O_2 + 5%H_2O/N_2 balanced).

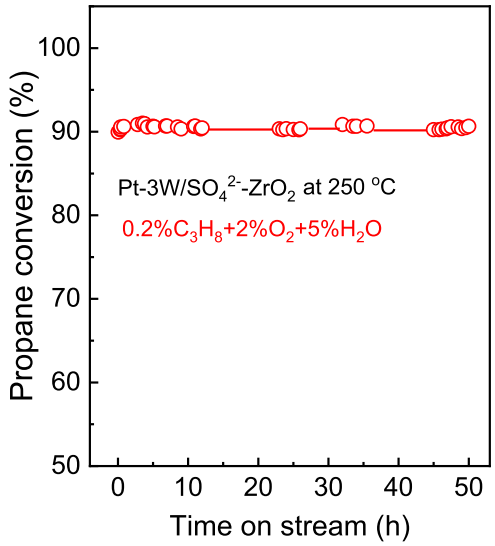

Fig. 3. Stability of the Pt-3W/SO_4^{2-}-ZrO_2 catalyst for propane oxidation with 5% H_2O vapor.

is consistent with its worse water tolerance as given in Fig. 2d. The Pt-3W/SO_4^{2-}-ZrO_2 catalyst shows a negative rate order of only − 0.13, explaining why water vapor only slightly affects its catalytic performance, particularly at high reaction temperature (>250 °C), as seen in Fig. 2d and Fig. S3. Such result represents the competitive adsorption on active sites is weakened on the Pt-3W/SO_4^{2-}-ZrO_2 catalyst, which should be related to its enhanced SMSI between Pt species and aggregated WO_3.

Apparent activation energies (Ea) of these catalysts under dry and wet conditions have been provided in Fig. 4d and Table S5. The much different apparent activation energies observed for these catalysts implies their very different activation ability for propane oxidation. Our previous work found that C-H bond of propane activated by Pt active sites is the rate determining step (RSD) for propane oxidation over the Pt/ZrO_2 catalyst (Ea=138.8 kJ mol^{-1}) under dry condition, whereas the C-C bond activated by synergistic catalysis of Pt and SO_4^{2-} is a new reaction pathway which remarkably decreases the apparent activation energy for propane oxidation reaction (Ea=36.3 kJ mol^{-1}).[43] The Pt-3W/SO_4^{2-}-ZrO_2 catalyst shows a Ea of 57.5 kJ mol^{-1} (Table S5) under dry condition, which is also much lower than that of the Pt/ZrO_2 catalyst. And the Pt-3W/SO_4^{2-}-ZrO_2 catalyst exhibits higher catalytic oxidation activity than the Pt-3W/ZrO_2 catalyst (Fig. 2), even though Pt-WO_3 interface site in WO_3 promoted Pt based catalyst is found to be very active sites for propane oxidation.[30] It is reasonable to infer that the reaction mechanism of propane oxidation over the Pt-3W/SO_4^{2-}-ZrO_2 catalyst is same to that on Pt/SO_4^{2-}-ZrO_2 catalyst, namely, C-C bond activated by synergistic catalysis of Pt and SO_4^{2-} is still the RSD. Under

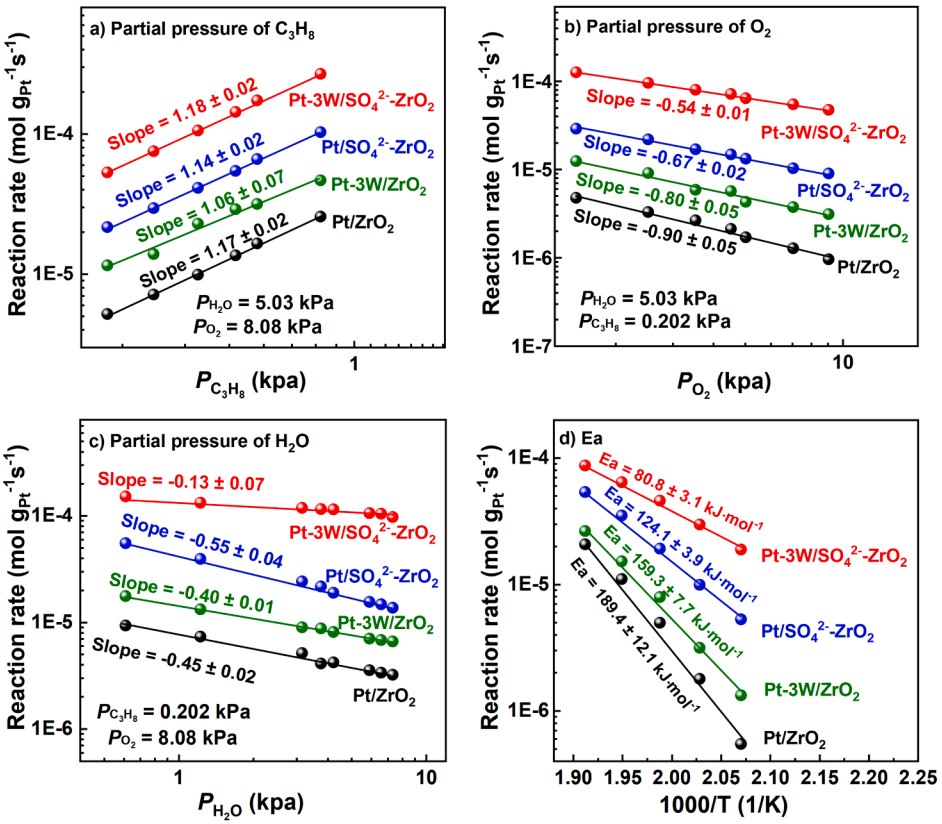

Fig. 4. Dependence of reaction rate on partial pressure of a) C_3H_8, b) O_2 and c) H_2O, and d) Arrhenius plots of Pt/ZrO_2, $Pt\text{-}3W/ZrO_2$, $Pt/SO_4^{2-}\text{-}ZrO_2$ and $Pt\text{-}3W/SO_4^{2-}\text{-}ZrO_2$ catalyst.

Table 2
Kinetic parameters of propane oxidation over Pt/ZrO_2, $Pt\text{-}3W/ZrO_2$, $Pt/SO_4^{2-}\text{-}ZrO_2$ and $Pt\text{-}3W/SO_4^{2-}\text{-}ZrO_2$ catalysts under wet condition.

Catalyst	$r = k\,[P_{C3H8}]^a\,[P_{O2}]^b[P_{H2O}]^c$				
	k ($\times 10^{-5}$)	a	b	c	Ea ($kJ{\cdot}mol^{-1}$)
Pt/ZrO_2	1.61	1.17 ± 0.02	-0.90 ± 0.05	-0.45 ± 0.02	189.4 ± 12.1
$Pt\text{-}3W/ZrO_2$	4.35	1.06 ± 0.07	-0.80 ± 0.05	-0.40 ± 0.01	159.3 ± 7.7
$Pt/SO_4^{2-}\text{-}ZrO_2$	13.43	1.14 ± 0.02	-0.67 ± 0.02	-0.55 ± 0.04	124.1 ± 3.9
$Pt\text{-}3W/SO_4^{2-}\text{-}ZrO_2$	48.33	1.18 ± 0.02	-0.54 ± 0.01	-0.13 ± 0.07	80.8 ± 3.1

wet condition, the increased apparent activation energies of all these catalysts in comparison with those under dry condition can be ascribed to the active sites poisoned by H_2O. For instance, Ea of the $Pt/SO_4^{2-}\text{-}ZrO_2$ catalyst significantly increases from 36.3 to 124.1 kJ mol^{-1}. This observation is related to the result of remarkable decrease of CO on Pt sites in the CO-DRIFTS spectra (Fig. 5) which will be discussed in following. Due to the enhanced SMSI effect, the Pt sites in the $Pt\text{-}3W/SO_4^{2-}\text{-}ZrO_2$ catalyst is highly water tolerant as confirmed by the CO-DRIFTS spectra (Fig. 5), thus, the Ea of the $Pt\text{-}3W/SO_4^{2-}\text{-}ZrO_2$ catalyst only increases from 57.7 to 80.8 kJ mol^{-1} (Table S5). The lowest apparent activation energy of $Pt\text{-}3W/SO_4^{2-}\text{-}ZrO_2$ catalyst confirms the propane could be easily activated on the $Pt\text{-}3W/SO_4^{2-}\text{-}ZrO_2$ catalyst surface under wet condition compared to the Pt/ZrO_2 $Pt\text{-}3W/ZrO_2$, and $Pt/SO_4^{2-}\text{-}ZrO_2$ catalysts. By comparing the kinetic results from dry and wet condition (Table S5), it can also be found that water vapor has negative effect.

on catalytic activity of these catalyst but only slightly affects the Pt-

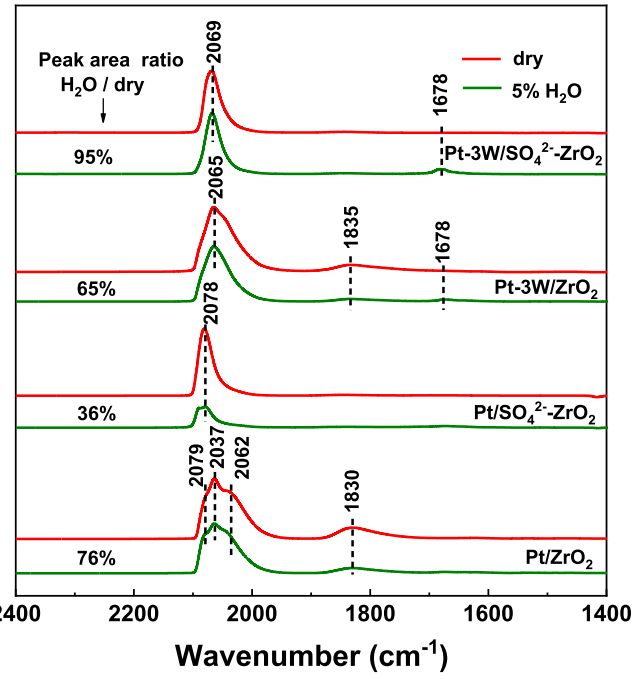

Fig. 5. CO-DRIFTS spectra of the Pt/ZrO_2, $Pt\text{-}3W/ZrO_2$, $Pt/SO_4^{2-}\text{-}ZrO_2$ and $Pt\text{-}3W/SO_4^{2-}\text{-}ZrO_2$ catalysts under dry or wet (5%H_2O) condition.

$3W/SO_4^{2-}\text{-}ZrO_2$ catalyst, especially for high reaction temperature (> 250 °C).

To further investigate water competitive absorption on active sites, CO-DRIFTS spectra of the catalysts were recorded under dry and wet

(5% H_2O) conditions, respectively, and their peak area ratios have been analyzed as shown in Fig. 5. CO probe molecule is used to perform the DRIFTS spectra instead of the propane owing to propane weak adsorption on Pt active sites.[5] The red and green profiles represent the CO-DRIFTS spectra recorded under dry and wet condition (5% H_2O), respectively. The Pt/ZrO_2 shows a wide band at 2000–2100 cm^{-1} which is ascribed to CO linearly adsorbed on Pt^0 sites, and a weak band at ~1800 cm^{-1} corresponds to bridged CO adsorption on Pt^0 sites. For the $Pt\text{-}3W/ZrO_2$ catalyst, the peak type of CO linearly adsorbed on Pt^0 sites slightly changes and bridged CO adsorption on Pt^0 sites disappears in comparison with those of the Pt/ZrO_2 catalyst. Moreover, no peak ascribed to bridged CO adsorption on Pt^0 sites can be found for both the $Pt/SO_4^{2-}\text{-}ZrO_2$ and $Pt\text{-}3W/SO_4^{2-}\text{-}ZrO_2$ catalysts, and a narrow band centered at ~ 2070 cm^{-1} is attributed to CO linearly adsorbed on Pt^0 sites, which is very different from those peaks of the Pt/ZrO_2 catalyst. The above results suggest WO_3 and SO_4^{2-} strongly interact with Pt sites and affect the CO adsorption on Pt sites. Additionally, it can be seen that the presence of water vapor would lead to the remarkable decrease of peak area in comparison with that recorded under dry condition for the Pt/ZrO_2, $Pt/SO_4^{2-}\text{-}ZrO_2$ and $Pt\text{-}3W/ZrO_2$ catalysts. This result suggests that the strongly competitive adsorption of water vapor on catalyst suppresses the CO adsorption. Especially for the $Pt/SO_4^{2-}\text{-}ZrO_2$ catalyst, based on the ratio of IR peak area collected under wet to dry, it can be considered that only 36% Pt sites are remained and accessible for CO adsorption under wet condition. This result can be ascribed to abundant hydrophilic strong acid sites in $Pt/SO_4^{2-}\text{-}ZrO_2$ catalyst. It is appealing to find that near 95% Pt sites in $Pt\text{-}3W/SO_4^{2-}\text{-}ZrO_2$ catalyst still accessible for CO adsorption under wet condition compared to that under dry condition, according to the ratio of peak area in Fig. 5. This result indicates most of Pt active sites in $Pt\text{-}3W/SO_4^{2-}\text{-}ZrO_2$ catalyst are water tolerant under such condition. Namely, the ability of competitive adsorption of H_2O on Pt active sites is remarkably weakened in Pt-3 $W/SO_4^{2-}\text{-}ZrO_2$ catalyst, the suppressed adsorption of small molecule (CO, H_2) on Pt species is the most pronounced character of reducible oxides supported Pt catalyst due to SMSI. Thus, it is reasonable to infer that the suppressed water adsorption on Pt active sites in $Pt\text{-}3W/SO_4^{2-}\text{-}ZrO_2$ should be ascribed to the enhanced SMSI between Pt species with reducible oxides WO_3. In addition, a very weak peak at 1678 cm^{-1} can be found in spectrum of $Pt\text{-}3W/ZrO_2$ catalyst recorded only under wet condition (5% H_2O), Amrollahi et al. assigned such characteristic peak to H_2O adsorption on WO_3 species surface in bending mode. [51] This peak is absent in spectra of Pt/ZrO_2 and $Pt/SO_4^{2-}\text{-}ZrO_2$ catalysts without WO_3 species. The intensity of this characteristic peak obviously increase for $Pt\text{-}3W/SO_4^{2-}\text{-}ZrO_2$ catalyst compared to $Pt\text{-}3W/ZrO_2$. Such result suggest that water vapor preferred to adsorb on aggregated WO_3 (in $Pt\text{-}3W/SO_4^{2-}\text{-}ZrO_2$) rather than monolayer WO_3 (in $Pt\text{-}3W/ZrO_2$).

Fig. 6 displays the Pt 4 f XPS spectra of fresh and spent (working under wet condition) catalysts to further understand the state of Pt species. Pt 4 f XPS spectra of fresh Pt/ZrO_2 and $Pt/SO_4^{2-}\text{-}ZrO_2$ catalysts can be deconvoluted into four components. The components with binding energies at 72.8 and 76.3 eV are attributed to Pt 4 $f_{7/2}$ and Pt 4 $f_{5/2}$ of Pt^{2+} species, respectively; and other two components with binding energies at 75.0 and 78.2 eV correspond to Pt 4 $f_{7/2}$ and Pt 4 $f_{5/2}$ of Pt^{4+} species, respectively. No components of Pt^0 species can be found for the fresh Pt/ZrO_2 and $Pt/SO_4^{2-}\text{-}ZrO_2$ catalysts. For the fresh $Pt\text{-}3W/ZrO_2$ and $Pt\text{-}3W/SO_4^{2-}\text{-}ZrO_2$ catalysts, new components assigned to Pt^0 species are observed at 71.5 and 74.9 eV which are assigned to Pt 4 $f_{7/2}$ and Pt 4 $f_{5/2}$ of Pt^0 species, respectively. This results confirm that WO_3 species promote the generation of Pt^0 species on catalyst surface. In addition, the $Pt\text{-}3W/SO_4^{2-}\text{-}ZrO_2$ catalyst has more Pt^0 species than the $Pt\text{-}3W/ZrO_2$ catalyst. It can be further inferred that PtO_x on aggregated WO_3 may be easier to be reduced in comparison with those on monolayer WO_3. For the spent catalysts, Pt^0 specie is still absent for the Pt/ZrO_2 catalyst but appears on the $Pt/SO_4^{2-}\text{-}ZrO_2$ catalyst. And the ratio of Pt^0 specie further increases for the $Pt\text{-}3W/ZrO_2$ and $Pt\text{-}3W/SO_4^{2-}\text{-}ZrO_2$ catalysts. The formation of Pt^0 species is certainly ascribed to the reduction of PtO_x induced by propane or its hydrocarbon intermediates during oxidation reaction process, which is consistent with previous works [5,43]. The above results suggest that the Pt species would restructure during propane oxidation. Our previous works confirm that increasing Pt^0 specie significantly enhanced propane oxidation activity of catalyst [26,52]. Therefore, the most Pt^0 specie observed on $Pt\text{-}3W/SO_4^{2-}\text{-}ZrO_2$ catalyst is responsible for its highest propane oxidation activity under wet condition. Although the $Pt\text{-}3W/ZrO_2$ catalyst shows a comparable Pt^0 specie compared to the $Pt/SO_4^{2-}\text{-}ZrO_2$ catalyst, the latter exhibits superior activity for propane oxidation due to the promotion of SO_4^{2-} group on C-C bond activation in propane as discussed in our previous work [43].

According to the above results, we proposed the relationship between catalyst structure and SMSI in the catalyst as shown in Scheme 1. No SMSI is observed in Pt/ZrO_2 because of its difficultly reducible oxides support ZrO_2. It is found that SMSI also does not take place in Pt-3W/

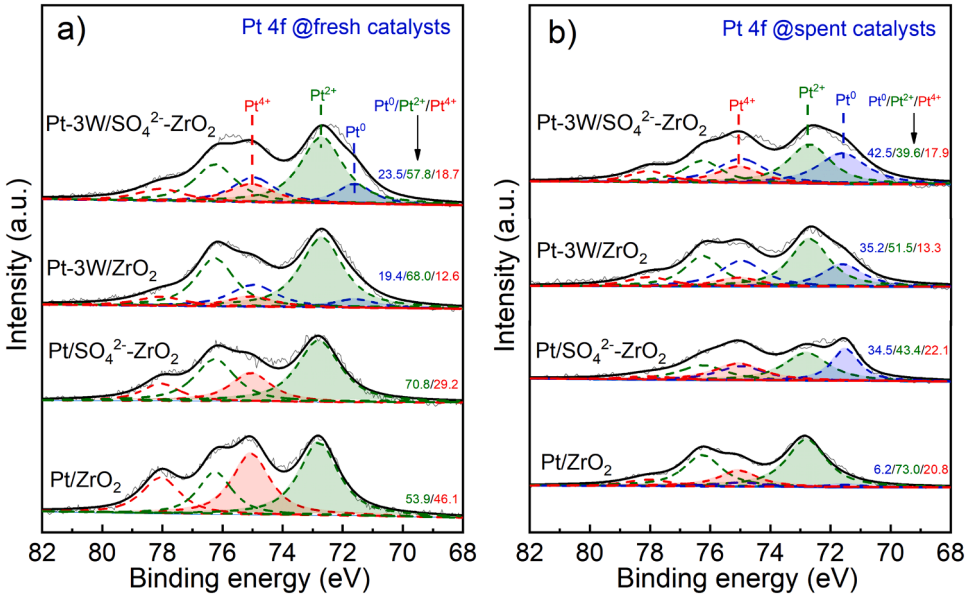

Fig. 6. XPS spectra Pt 4 f of the Pt/ZrO_2, $Pt\text{-}3W/ZrO_2$, $Pt/SO_4^{2-}\text{-}ZrO_2$ and $Pt\text{-}3W/SO_4^{2-}\text{-}ZrO_2$ catalysts.

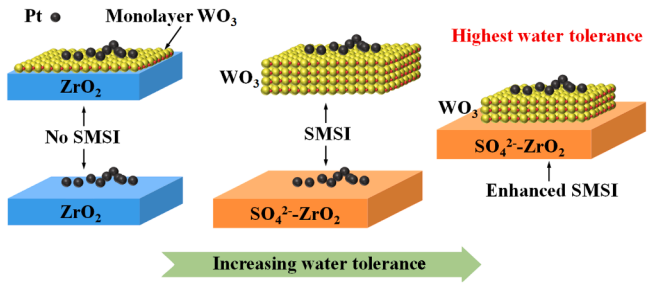

Scheme 1. Proposed case of SMSI in the Pt/ZrO_2, Pt/WO_3, $Pt\text{-}3W/ZrO_2$, $Pt/SO_4^{2-}\text{-}ZrO_2$ and $Pt\text{-}3W/SO_4^{2-}\text{-}ZrO_2$ catalysts.

ZrO_2 due to the monolayer dispersed WO_3 structure. It can be found the SMSI exists in the Pt/WO_3 and $Pt/SO_4^{2-}\text{-}ZrO_2$ catalysts, in which the CO chemical adsorption is seriously suppressed. For the $Pt\text{-}3W/SO_4^{2-}\text{-}ZrO_2$ catalyst, the SMSI is enhanced and the CO chemical adsorption is further suppressed (Table 1). The SMSI in the catalyst not only suppresses the CO adsorption but also the water vapor adsorption on the active sites based on the results of CO-DRIFTS spectra and kinetic experiments, thus, the enhanced SMSI in the $Pt\text{-}3W/SO_4^{2-}\text{-}ZrO_2$ catalyst results in the highest water tolerance.

4. Conclusion

In summary, we designed an novel $Pt\text{-}3W/SO_4^{2-}\text{-}ZrO_2$ catalyst with high activity and water tolerance for propane complete oxidation. It is found that monolayer WO_3 generate in $Pt\text{-}3W/ZrO_2$ catalyst whereas the aggregated WO_3 species is observed in $Pt\text{-}3W/SO_4^{2-}\text{-}ZrO_2$ catalyst. SMSI between WO_3 and Pt species can be found in Pt/WO_3 but such interaction disappears in $Pt\text{-}3W/ZrO_2$ catalyst with monolayer WO_3. Furthermore, such SMSI is further enhanced in $Pt\text{-}3W/SO_4^{2-}\text{-}ZrO_2$ catalyst with aggregated WO_3, which plays critical role on weakening the water vapor competitive adsorption on active sites. Thus, the $Pt\text{-}3W/SO_4^{2-}\text{-}ZrO_2$ catalyst not only exhibits excellent oxidation activity but also robust water tolerance for propane complete oxidation.

CRediT authorship contribution statement

Xu-Fang Wang: Conceptualization, Data curation, Formal analysis, Investigation, Software, Visualization, Writing – original draft. **Lin-Ya Xu:** Conceptualization, Data curation, Formal analysis, Investigation. **Cai-Hao Wen**: Investigation, Data curation, Formal analysis, Visualization. **Dan-Dan Li:** Conceptualization, Investigation, Resources, Data curation, Funding acquisition. **Bei Li:** Software, Visualization, Funding acquisition. **Qi-Hua Yang:** Conceptualization, Investigation, Formal analysis, Resources, Writing – review & editing. **Ji-Qing Lu:** Conceptualization, Investigation, Formal analysis, Resources. **Mengfei Luo:** Conceptualization, Data curation, Formal analysis, Funding acquisition, Investigation, Methodology, Resources, Project administration, Supervision, Writing – review & editing. **Jian Chen**: Conceptualization, Data curation, Formal analysis, Investigation, Visualization, Software, Methodology, Supervision, Writing – review & editing.

Declaration of Competing Interest

The authors declare that they have no known competing financial interests or personal relationships that could have appeared to influence the work reported in this paper.

Data Availability

Data will be made available on request.

Acknowledgements

This work was financially supported by the National Natural Science Foundation of China (No. 22172145, 22072137, 21902146).

Appendix A. Supporting information

Supplementary data associated with this article can be found in the online version at doi:10.1016/j.apcatb.2023.123000.

References

[1] Y. Shen, J. Deng, X. Hu, X. Chen, H. Yang, D. Cheng, D. Zhang, Expediting toluene combustion by harmonizing the Ce-O strength over Co-doped CeZr oxide catalysts, Environ. Sci. Technol. 57 (2023) 1797–1806.
[2] Y. Shen, J. Deng, L. Han, W. Ren, D. Zhang, Low-temperature combustion of toluene over Cu-doped $SmMn_2O_5$ mullite catalysts via creating highly active Cu^{2+}-O-Mn^{4+} sites, Environ. Sci. Technol. 56 (2022) 10433–10441.
[3] Y. Shen, J. Deng, S. Impeng, S. Li, T. Yan, J. Zhang, L. Shi, D. Zhang, Boosting toluene combustion by engineering Co-O strength in cobalt oxide catalysts, Environ. Sci. Technol. 54 (2020) 10342–10350.
[4] S. Wang, S. Wang, X. Zong, S. Wang, X. Dong, CO oxidation with Pt catalysts supported on different supports: a comparison of their sulfur tolerance properties, Appl. Catal. A Gen. 654 (2023), 119083.
[5] X. Wang, C. Liu, L. He, B. Li, J. Lu, M. Luo, J. Chen, Unveiling geometric and electronic effects of Pt species on water-tolerant Pt/ZSM-5 catalyst for propane oxidation, Appl. Catal. A Gen. 655 (2023), 119108.
[6] H.S. Gandhi, G.W. Graham, R.W. McCabe, Automotive exhaust catalysis, J. Catal. 216 (2003) 433–442.
[7] J.Y. Luo, M. Meng, Y.Q. Zha, L.H. Guo, Identification of the active sites for CO and C_3H_8 total oxidation over nanostructured $CuO\text{-}CeO_2$ and $Co_3O_4\text{-}CeO_2$, Catal., J. Phys. Chem. C. 112 (2008) 8694–8701.
[8] B. Li, X.F. Wang, W.Y. Wang, C.F. Liu, L.C. He, M.F. Luo, J. Chen, Identifying the surface active sites of FeO_x-modified Pt/Nb_2O_5 catalysts in CO and propane oxidation, Appl. Catal. A Gen. 649 (2023), 118960.
[9] B. Cen, P. Zhao, J. Chen, M. Luo, The role of Ba additive on the catalytic performance of Pd/Al_2O_3 and Pt/Al_2O_3 for $C_1\text{-}C_3$ alkanes deep oxidation, Ind. Catal. 28 (2020) 89–94.
[10] Y. Yazawa, N. Takagi, H. Yoshida, S. Komai, A. Satsuma, T. Tanaka, S. Yoshida, T. Hattori, The support effect on propane combustion over platinum catalyst: Control of the oxidation-resistance of platinum by the acid strength of support materials, Appl. Catal. A Gen. 233 (2002) 103–112.
[11] Y. Yazawa, H. Yoshida, T. Hattori, The support effect on platinum catalyst under oxidizing atmosphere: improvement in the oxidation-resistance of platinum by the electrophilic property of support materials, Appl. Catal. A Gen. 237 (2002) 139–148.
[12] Y. Yazawa, H. Yoshida, S. Komai, T. Hattori, The additive effect on propane combustion over platinum catalyst: control of the oxidation-resistance of platinum by the electronegativity of additives, Appl. Catal. A Gen. 233 (2002) 113–124.
[13] M. Kobayashi, A. Morita, M. Ikeda, The support effect in oxidizing atmosphere on propane combustion over platinum supported on TiO_2, TiO2-SiO2 and TiO2-SiO2-WO3, Appl. Catal. B Environ. 71 (2007) 94–100.
[14] H. Yoshida, Y. Yazawa, T. Hattori, Effects of support and additive on oxidation state and activity of Pt catalyst in propane combustion, Catal. Today 87 (2003) 19–28.
[15] G. Corro, J.L.G. Fierro, V.C. Odilon, An XPS evidence of Pt4+ present on sulfated Pt/Al2O3 and its effect on propane combustion, Catal. Commun. 2003, 4, 371–376.
[16] C. Shao, Y. Cui, L. Zhang, J. Tang, C. Ge, B. Chen, L. Wang, Y. Guo, W. Zhan, Y. Guo, Boosting propane purification on $Pt/ZrOSO_4$ nanoflowers: Insight into the roles of different sulfate species in synergy with Pt, Sep. Purif. Technol. 304 (2023), 122367.
[17] H. Hao, B. Jin, W. Liu, X. Wu, F. Yin, S. Liu, Robust $Pt@TiO_x/TiO_2$ catalysts for hydrocarbon combustion: Effects of Pt-TiO_x interaction and sulfates, ACS Catal. 10 (2020) 13543–13548.
[18] L. Zhang, D. Weng, B. Wang, X. Wu, Effects of sulfation on the activity of Ce0.67Zr0.33O2 supported Pt catalyst for propane oxidation, Catal. Commun. 11 (15) (2010) 1229–1232.
[19] L. Gu, X. Chen, Y. Zhou, Q. Zhu, H. Huang, H. Lu, Propene and CO oxidation on $Pt/Ce\text{-}Zr\text{-}SO_4^{2-}$ diesel oxidation catalysts: Effect of sulfate on activity and stability, Chin. J. Catal. 38 (2017) 607–616.
[20] X.D. Wu, Z. Zhou, D. Weng, B. Wang, Effects of tungsten oxide on the activity and thermal stability of a sulfate-derived titania supported platinum catalyst for propane oxidation, J. Environ. Sci. 24 (2012) 458–463.
[21] M. Skoglundh, A. Ljungqvist, M. Petersson, E. Fridell, Neil Cruise, O. Augustsson, E. Jobson, SO_2 promoted oxidation of ethyl acetate, ethanol and propane, Appl. Catal. B Environ. 30 (2001) 315–328.
[22] A.F. Lee, K. Wilson, R.M. Lambert, C.P. Hubbard, R.G. Hurley, R.W. McCabe, H. S. Gandhi, The origin of SO_2 promotion of propane oxidation over Pt/Al_2O_3 catalysts, J. Catal. 184 (1999) 491–498.
[23] A. Hinz, M. Skoglundh, E. Fridell, A. Andersson, An investigation of the reaction mechanism for the promotion of propane oxidation over Pt/Al_2O_3 by SO_2, J. Catal. 201 (2) (2001) 247–257.

[24] K. Wilson, C. Hardacre, R.M. Lambert, SO_2-promoted, chemisorption and oxidation of propane over Pt (111), J. Phys. Chem. 99 (38) (1995) 13755–13758.
[25] J.E. Park, K.B. Kim, K.S. Song, Y.A Kim, E.D. Park, Effect of Pt particle size on propane combustion over Pt/ZSM-5, Catal. Lett. 143 (2013) 1132–1138.
[26] P. Zhao, J. Chen, H. Yu, B. Cen, W. Wang, M. Luo, J. Lu, Insights into propane combustion over MoO_3 promoted Pt/ZrO_2 catalysts: the generation of Pt-MoO_3 interface and its promotional role on catalytic activity, J. Catal. 391 (2020) 80–90.
[27] P. Zhao, W. Wang, X. Wang, C. Liu, J. Lu, M. Luo, J. Chen, The effects of MoO_3 impregnation order on the catalytic activity for propane combustion over Pt/ZrO_2 catalysts: the crucial roles of Pt-MoO_3 interfacial sites density, N. J. Chem. 45 (2021) 14695–14702.
[28] P. Zhao, X. Li, W. Liao, Y. Wang, J. Chen, J. Lu, M. Luo, Understanding the role of NbO_x on Pt/Al_2O_3 for effective catalytic propane oxidation, Ind. Eng. Chem. Res. 58 (2019) 21945–21952.
[29] B. Cen, C. Tang, J. Lu, J. Chen, M. Luo, Different roles of MoO_3 and Nb_2O_5 promotion in short-chain alkane combustion over Pt/ZrO_2 catalysts, Chin. J. Catal. 42 (2021) 2287–2295.
[30] W. Liao, X. Fang, B. Cen, J. Chen, Y. Liu, M. Luo, J. Lu, Deep oxidation of propane over WO_3-promoted Pt/BN catalysts: the critical role of Pt-WO_3 interface, Appl. Catal. B Environ. 272 (2020), 118858.
[31] W.M. Liao, Y.R. Liu, P.P. Zhao, B.H. Cen, C. Tang, A.P. Jia, J.Q. Lu, M.F. Luo, Total oxidation of propane over Pt-V/SiO_2 catalysts: remarkable enhancement of activity by vanadium promotion, Appl. Catal. A Gen. 590 (2020), 117337.
[32] X. Wu, L. Zhang, D. Weng, S. Liu, Z. Si, J. Fan, Total oxidation of propane on Pt/WO_x/Al_2O_3 catalysts by formation of metastable $Pt_i^{\delta+}$ species interacted with WO_x clusters, J. Hazard. Mater. 225–226 (2012) 146–154.
[33] Z. Zhu, G. Lu, Y. Guo, Y. Guo, Z. Zhang, Y. Wang, X. Gong, High performance and stability of the Pt-W/ZSM-5 catalyst for the total oxidation of propane: the role of tungsten, ChemCatChem 5 (2013) 2495–2503.
[34] B. Han, Y. Guo, Y. Huang, W. Xi, J. Xu, J. Luo, H. Qi, Y. Ren, X. Liu, B. Qiao, T. Zhang, Strong metal-support interactions between Pt single stoms and TiO_2, Angew. Chem. Int. Ed. 59 (2020) 11824–11829.
[35] L. Lin, S. Yao, R. Gao, X. Liang, Q. Yu, Y. Deng, J. Liu, M. Peng, Z. Jiang, S. Li, Y. Li, X. Wen, W. Zhou, D. Ma, A highly CO-tolerant atomically dispersed Pt catalyst for chemoselective hydrogenation, Nat. Nanotechnol. 14 (2019) 354–361.
[36] Q. Dai, Q. Zhu, Y. Lou, X. Wang, Role of Brønsted acid site during catalytic combustion of methane over PdO/ZSM-5: dominant or negligible? J. Catal. 357 (2018) 29–40.
[37] K. Murata, J. Ohyama, Y. Yamamoto, S. Arai, A. Satsuma, Methane combustion over Pd/Al_2O_3 catalysts in the presence of water: effects of Pd particle size and alumina crystalline phase, ACS Catal. 10 (2020) 8149–8156.
[38] W. Huang, X. Zhang, A. Yang, E.D. Goodman, K. Kao, M. Cargnello, Enhanced catalytic activity for methane combustion through in situ water sorption, ACS Catal. 10 (2020) 8157–8167.
[39] A. Yang, H. Zhu, Y. Li, M. Cargnello, Support acidity improves Pt activity in propane combustion in the presence of steam by reducing water coverage on the active sites, ACS Catal. 11 (2021) 6672–6683.
[40] N.M. Kinnunen, J.T. Hirvi, K. Kallinen, T. Maunula, M. Keenan, M. Suvanto, Case study of a modern lean-burn methane combustion catalyst for automotive applications: what are the deactivation and regeneration mechanisms ? Appl. Catal. B Environ. 207 (2017) 114–119.
[41] H. Xiong, M.H. Wiebenga, C. Carrillo, J.R. Gaudet, H.N. Pham, D. Kunwar, S.H. Oh, G. Qi, C.H. Kim, A.K. Datye, Design considerations for low-temperature hydrocarbon oxidation reactions on Pd based catalysts, Appl. Catal. B Environ. 236 (2018) 436–444.
[42] J. Yang, M. Peng, G. Ren, H. Qi, X. Zhou, J. Xu, F. Deng, Z. Chen, J. Zhang, K. Liu, X. Pan, W. Liu, Y. Su, W. Li, B. Qiao, D. Ma, T. Zhang, A hydrothermally stable irreducible oxide-modified $Pd/MgAl_2O_4$ catalyst for methane combustion, Angew. Chem. Int. Ed. 59 (2020) 18522–18526.
[43] D.D. Li, X.Y. Leng, X.F. Wang, H.B. Yu, W.Q. Zhang, J. Chen, J.Q. Lu, M.F. Luo, Unraveling the promoting roles of sulfate groups on propane combustion over Pt-SO_4^{2-}/ZrO_2 catalysts, J. Catal. 407 (2022) 322–332.
[44] S.J. Tauster, S.C. Fung, R.L. Garten, Strong metal-support interactions. Group 8 noble metals supported on TiO_2, J. Am. Chem. Soc. 100 (1978) 170–175.
[45] P.D.L. Mercera, J.G. Van Ommen, E.B.M. Doesburg, A.J. Burggraaf, J.R.H. Ross, Zirconia as a support for catalysts: evolution of the texture and structure on calcination in air, Appl. Catal. 57 (1990) 127–148.
[46] P. Wang, S. Wei, S. Wang, R. Lin, X. Mou, Y. Ding, Interface-directed epitaxially growing nickle ensembles as efficient catalysts in dry reforming of methane, J. Energy Chem. 66 (2022) 502–513.
[47] D. Nedumaran, A. Pandurangan, Effect of tungsten loading on zirconia impregnated MCM-41 and its catalytic activity on transesterification reaction, J. Porous Mater. 20 (2013) 897–908.
[48] W. Sun, Z. Zhao, C. Guo, X. Ye, Y. Wu, Study of the alkylation of isobutane with n-butene over WO_3/ZrO_2 strong solid acid. 1. Effect of the preparation method, WO_3 loading, and calcination temperature, Ind. Eng. Chem. Res. 39 (10) (2000) 3717–3725.
[49] T. Nishiguchi, K. Oka, T. Matsumoto, H. Kanai, K. Utani, S. Imamura, Durability of WO_3/ZrO_2-CuO/CeO_2 catalysts for steam reforming of dimethyl ether, Appl. Catal. A Gen. 301 (2006) 66–74.
[50] L. Dixit, D.L. Gerrard, H.J. Bowley, Laser Raman spectra of transition metal oxides and catalysts, Appl. Spectrosc. Rev. 22 (1986) 189–249.
[51] R. Amrollahi, K. Wenderich, G. Mul, Room temperature oxidation of ethanol to acetaldehyde over Pt/WO_3, Adv. Mater. Interfaces 3 (2016) 1600266.
[52] Y. Liu, X. Li, W. Liao, A. Jia, Y. Wang, M. Luo, J. Lu, Highly active Pt/BN catalysts for propane combustion: the roles of support and reactant-induced evolution of active sites, ACS Catal. 9 (2019) 1472–1481.